Inorg. Chem. **2008**, *47*, 1428−1434

Synthesis of Discrete and Dispersible MoS_2 Nanocrystals

Hongtao Yu, Yi Liu, and Stephanie L. Brock*

Department of Chemistry, Wayne State University, Detroit, Michigan 48202

Received May 25, 2007

MoS_2 nanoparticles of size <5 nm have been synthesized via the reaction of $Mo(CO)_6$ with elemental sulfur in trioctylphosphine oxide and 1-octadecene at temperatures from 270 to 330 °C. The MoS_2 nanoparticles are discrete and dispersible in a variety of nonpolar organic solvents, including toluene, chloroform, and pyridine. The size of the particles can be effectively tuned by varying the temperature, yielding nearly monodisperse samples (<10% standard deviation) as evidenced by transmission electron microscopy (TEM). Additionally, larger (20–50 nm) onion- and tube-shaped MoS_2 nanoparticles can be obtained by decreasing the amount of the coordinating solvent (trioctylphosphine oxide) relative to 1-octadecene. As-prepared samples are poorly crystalline, showing only weak contrast in the TEM and an absence of the first-order (00*l*) reflection in powder X-ray diffraction that is indicative of regular MoS_2 stacking. Samples heated in situ in the TEM are observed to develop contrast and lattice fringes as the temperature is raised to 550 °C. Ex-situ heated samples show the appearance of the first order (00*l*) reflection at temperatures >870 °C.

Introduction

Molybdenum disulfide nanomaterials have received considerable attention from the materials community due to the catalytic activity of alumina supported MoS_2. These materials are employed commercially for hydrodesulfurization of fossil fuels. The traditional synthesis of the Al_2O_3 supported catalyst involves simultaneous impregnation of molybdenum and promoter (Co, Ni) salts onto alumina, followed by calcination and sulfidation. While this approach has been effective, it offers little control over the particle size and morphology of the active phase. Accordingly, there has been intense interest in the controlled synthesis of nanometer scale MoS_2 materials, since smaller particles can be expected to have a larger percentage of active (edge) sites.[1] Additionally, such materials can be expected to exhibit quantum confinement effects when prepared with sizes less than the Bohr radius of the exciton (electron–hole pair, 4 nm for MoS_2).

Aside from the formation of supported catalysts, there are two general synthetic approaches to MoS_2 nanoparticles: physical and chemical methods. Physical methods typically involve a high-energy technique such as microwave plasma,[2] laser ablation,[3] arc discharge,[4,5] or pulsed-laser vaporization.[6,7] These methods are rapid but the resultant MoS_2 nanoparticles are bare and tend to form aggregates, reducing surface areas and precluding further functionalization or dispersion.

Chemical syntheses of MoS_2 nanoparticles have been achieved by a wide range of methods, including metal−organic chemical vapor deposition; high-temperature transport, decomposition or annealing strategies; inverse micelle; solvothermal; and sonochemical syntheses. Tremel and co-workers developed a metal−organic chemical vapor deposition method to synthesize crystalline inorganic-fullerene-type MoS_2 nanoparticles between 10 and 40 nm.[8] However, the size monodispersity of a single reaction was relatively large, and the resultant nanoparticle aggregates had to be treated with polydentate water-soluble polymers to effect dispersion

* To whom correspondence should be addressed. E-mail: sbrock@chem.wayne.edu.

(1) Kushmeerick, J. G.; Weiss, P. S. *J. Phys. Chem. B* **1998**, *102*, 10094–10097.
(2) Vollath, D.; Szabo, D. V. *Acta Mater.* **2000**, *48*, 953.
(3) Sen, R.; Govindaraj, A.; Suenaga, K.; Suzuki, S.; Kataura, H.; Iijima, S.; Achiba, Y. *Chem. Phys. Lett.* **2001**, *340*, 242–248.
(4) Sano, N.; Wang, H.; Chhowalla, M.; Alexandrou, I.; Amaratunga, G. A. J.; Heben, M. J. *Chem. Phys. Lett.* **2003**, *368*, 331–337.
(5) Chhowalla, M.; Amaratunga, G. A. J. *Nature* **2000**, *407*, 164–167.
(6) Parilla, P. A.; Dillon, A. C.; Jones, K. M.; Riker, G.; Schulz, D. L.; Ginley, D. S.; Heben, M. J. *Nature* **1999**, *397*, 114.
(7) Parilla, P. A.; Dillon, A. C.; Parkinson, B. A.; Jones, K. M.; Alleman, J.; Riker, G.; Ginley, D. S.; Heben, M. J. *J. Phys. Chem. B* **2004**, *108*, 6197–6207.
(8) Etzkorn, J.; Therese, H. A.; Rocker, F.; Zink, N.; Kolb, U.; Tremel, W. *Adv. Mater.* **2005**, *17*, 2372.

10.1021/ic701020s CCC: $40.75 © 2008 American Chemical Society
Published on Web 02/08/2008

in aqueous solution.[9] Sonochemical approaches to MoS_2 nanoparticles employing $Mo(CO)_6$ and sulfur[10] resulted in 15–20 nm particles of amorphous MoS_2 that showed a higher catalytic activity for hydrodesulfurization (HDS) reactions than conventional RuS_2, ReS_2, and MoS_2.[11,12] Solvothermal methods have also resulted in poorly crystalline or totally amorphous products, poor control of size and shape, and poor solvent dispersity.[13,14] Hollow microspheres or nanotubes can be accessed from thermal decomposition of MoS_x ($3 < x < 6$).[15–17] Nanotubes are likewise prepared by thermal transport methods using C_{60} as a catalyst,[18] and fullerene-type MoS_2 is prepared by transformation of MoO_3 nanoparticles under H_2S/H_2 thermal treatment.[19]

Despite considerable attention to the synthesis of MoS_2 nanoparticles and nanostructures, only the inverse micelle approach enables very small particles (<10 nm), with narrow polydispersities to be prepared.[20–22] We surmised that the use of high temperature methods involving coordinating solvents, commonly employed in other nanoparticle syntheses, might enable monodisperse samples of MoS_2 to be prepared as well. Indeed, the formation of nanoparticles of MoS_2 from reaction of $Mo(CO)_6$ and sulfur has been demonstrated in a noncoordinating solvent (*para*-xylene) but the products are highly aggregated.[23] Here, we report a new and simple synthesis of discrete and dispersible MoS_2 nanoparticles by employing the coordinating solvent TOPO (trioctylphosphine oxide) as a synthetic medium. Experimental results show that while the as-obtained MoS_2 nanoparticles are poorly crystalline, samples can be prepared that exhibit a size distribution of less than 10% without further size selective precipitation.[24] Additionally, different shapes of MoS_2 nanocrystals can be obtained by changing the ratio of coordinating solvent (TOPO) and noncoordinating solvent (1-octadecene, ODE). Importantly, this method exploits commercially available $Mo(CO)_6$ and, thus, does not require preliminary synthesis of the precursor, as is the case for the inverse micellar route where $MoCl_4$ is employed. Thus, this new approach enables facile synthesis of very small MoS_2 nanoparticles (<5 nm) with low polydispersity, or larger multilayered structures, all by using commercially available precursors and a standard method. In keeping with previous studies,[11,12] the low crystallinity of the as-prepared samples can be expected to result in enhanced HDS activity, whereas the dispersibility of the particles should enable facile casting onto supports for catalyst preparation.

(9) Tahir, M. N.; N. Zink, M. E.; Therese, H. A.; Kolb, U.; Theato, P.; Tremel, W. *Angew. Chem., Int. Ed.* **2006**, *45*, 4809.
(10) Mdleleni, M. M.; Hyeon, T.; Suslick, K. S. *J. Am. Chem. Soc.* **1998**, *120*, 6189.
(11) Mahajan, D.; Marshall, C. L.; Castagnola, N.; Hanson, J. C. *Appl. Catal., A* **2004**, *258*, 83–91.
(12) Mastai, Y.; Homyonfer, M.; Gedanken, A.; Hodes, G. *Adv. Mater.* **1999**, *11*, 1010–1013.
(13) Berntsen, N.; Gutjahr, T.; Loeffler, L.; Gomm, J. R.; Seshadri, R.; Tremel, W. *Chem. Mater.* **2003**, *15*, 4498.
(14) Peng, Y.; Meng, Z.; Ahong, C.; Lu, J.; Yang, Z.; Qian, Y. *Mater. Chem. Phys.* **2002**, *73*, 327–329.
(15) Afanasiev, P.; Bezverkhy, I. *Chem. Mater.* **2002**, *14*, 2826–2830.
(16) Nath, M.; Govindaraj, A.; Rao, C. N. R. *Adv. Mater.* **2001**, *13*, 283–286.
(17) Xiong, Y.; Xie, Y.; Li, Z.; Li, X.; Zhang, R. *Chem. Phys. Lett.* **2003**, *382*, 180–185.
(18) Remskar, M.; Mrzel, A.; Skraba, Z.; Jesih, A.; Ceh, M.; Demsar, J.; Stadelmann, P.; Lévy, F.; Mihailovic, D. *Science* **2001**, *292*, 479–481.
(19) Feldman, Y.; Frey, G. L.; Homyonfer, M.; Lyakhovitskaya, V.; Margulis, L.; Cohen, H.; Hodes, G.; Hutchinson, J. L.; Tenne, R. *J. Am. Chem. Soc.* **1996**, *118*, 5362.
(20) Chikan, V.; Kelley, D. F. *J. Phys. Chem. B* **2002**, *106*, 3794–3804.
(21) Wilcoxon, J. P.; Newcomer, P. P.; Samara, G. A. *J. Appl. Phys.* **1997**, *81*, 7934.
(22) Wilcoxon, J. P.; Samara, G. A. *Phys. Rev. B* **1995**, *51*, 7299–7302.
(23) Duphil, D.; Bastide, S.; Levy-Clement, C. *J. Mater.Chem.* **2002**, *12*, 2430.
(24) Murray, C. B.; Kagan, C. R.; Bawendi, M. G. *Annu. Rev. Mater. Sci.* **2000**, *30*, 545–610.

Experimental Details

Materials. Molybdenum hexacarbonyl ($Mo(CO)_6$, 98%) and elemental sulfur (99.999%) were purchased from Strem. 1-Octadecene (ODE, 90%) was purchased from Acros. Trioctylphosphine oxide (TOPO, 90%) was purchased from Aldrich. Toluene, methanol, hexane, and pyridine were purchased from Fisher. All chemicals were used as received.

Synthesis of Sphere-Shaped MoS_2 Nanoparticles. Nearly monodisperse MoS_2 nanocrystals were synthesized via the reaction of $Mo(CO)_6$ with elemental sulfur in trioctylphosphine oxide at elevated temperature (270–330 °C). All manipulations were performed using standard air-free techniques. The sulfur precursor solution was prepared by dissolving elemental sulfur in 1-octadecene (ODE, 0.0085 g/mL) at 130 °C, then cooling down to 60 °C. A typical synthesis involved mixing $Mo(CO)_6$ (0.1056 g) with TOPO (10 g) in a flask, flushing the system with Ar, increasing the temperature to 250 °C, and maintaining the reaction at 250 °C overnight. The temperature was then raised to the target temperature (270, 300, 330 °C), and 3.0 mL of the sulfur/1-octadecene solution was rapidly injected into the reaction system. The reaction was maintained at the target temperature for 24 or 48 h and then cooled down to 60 °C, and 8.0 mL of toluene was injected into the system. The dispersion was subsequently cooled down to room temperature, and the MoS_2 nanoparticles were isolated by adding excess anhydrous methanol, centrifuging the mixture, and then removing the supernatant. The products could be further purified by dispersing the precipitate into 5.0 mL of toluene and then reprecipitating in an excess of methanol.

Synthesis of Onion- and Tube-Shaped MoS_2 Nanoparticles. A 0.2112 g portion of $Mo(CO)_6$ was mixed with 7 g TOPO in a flask, purged with Ar at room temperature, then heated to 250 °C, and left overnight. The temperature was then raised to 280 °C, and 10 mL of a sulfur/ODE solution (0.00512 g/mL) was rapidly injected into the system. The reaction was maintained at 280 °C for 24 h. The isolation and purification was conducted analogously to the sphere-shaped nanoparticles.

X-ray Powder Diffraction. X-ray powder diffraction data were acquired on a Rigaku RU 200B X-ray diffractometer (40 kV, 100 mW, Cu Kα radiation) with a rotating anode. Powder samples were spread on a thin film of grease on a low background holder composed of (0001) quartz for analysis. Alternatively, dispersed particles in toluene were deposited on the holder, followed by solvent evaporation. Samples were identified by comparison to phases in the International Centre for Diffraction Data (ICDD) powder diffraction file (PDF) database.

Transmission Electron Microscopy. Data were acquired on a JEOL 2010 FasTEM microscope operating at an accelerating voltage of 200 kV. Samples were prepared by depositing a drop of a toluene dispersion of MoS_2 nanocrystals on a carbon film supported by a 200–300 mesh copper grid and subsequently evaporating the solvent. The average particle size and standard

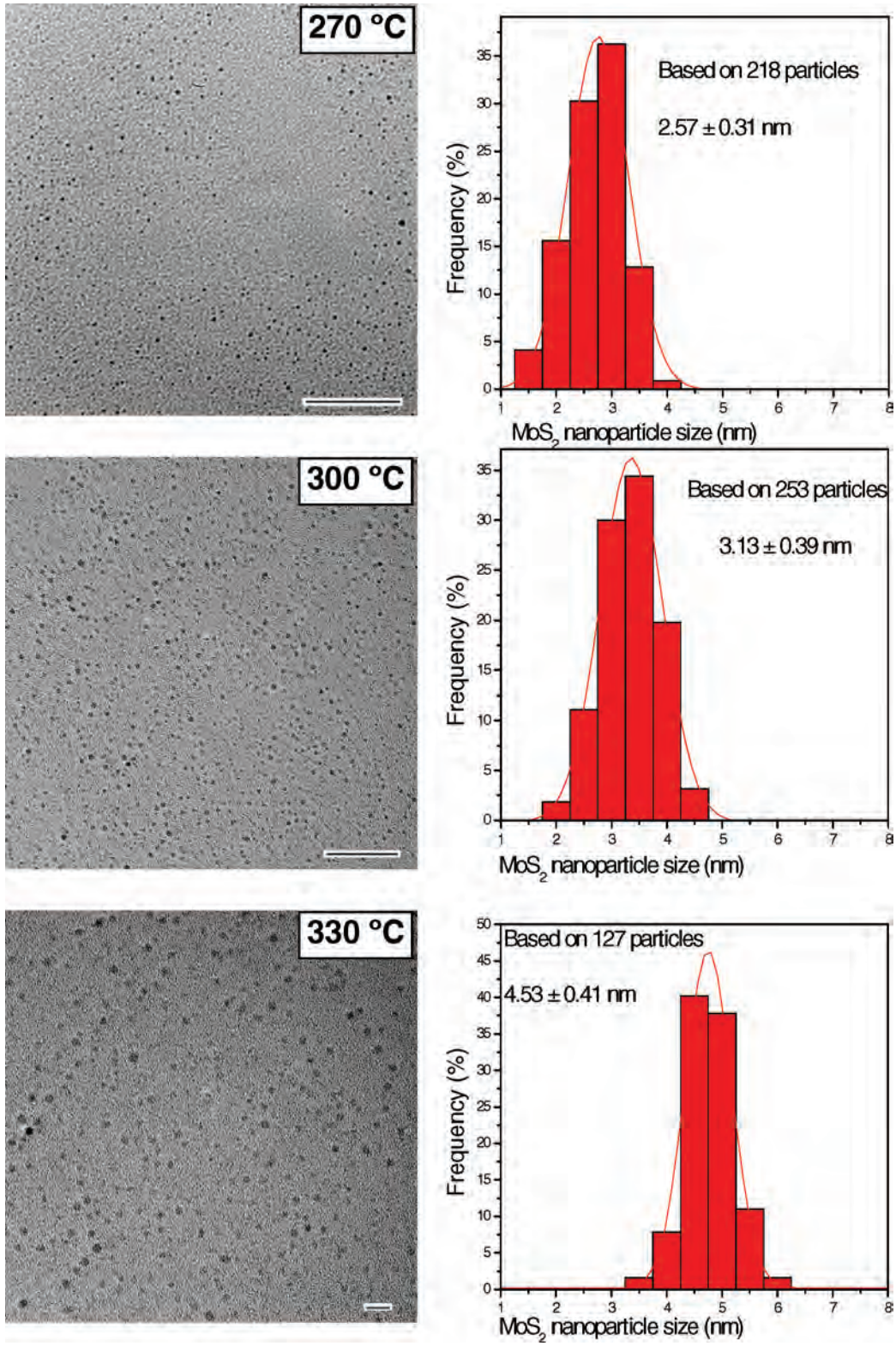

Figure 1. Low magnification TEM images of a field of MoS_2 nanoparticles prepared at different temperatures (48 h heating, left) and their corresponding size histograms (right). The scale bar is 100 nm for the 270 and 300 °C samples and 20 nm for the 330 °C sample. Due to low crystallinity and thus contrast, the electron beam was defocused to acquire these images.

deviation were determined from measurements (by hand on printed images) of over 100 particles. Relatively concentrated samples were used for selected area electron diffraction (SAED) measurements. Qualitative elemental compositions were obtained using an in situ energy dispersive spectroscopy (EDS) unit (EDAX, Inc.) attached to the transmission electron microscope. In-situ heating studies were performed in the transmission electron microscope (TEM) by using a Gatan double-tilt heating stage. The temperature was controlled using a 901 SmartSet Hot Stage Controller (Gatan Inc.). The heating rate was 10 °C/min.

Inductively Coupled Plasma (ICP) Chemical Analysis. Quantitative assessment of Mo and S contents were determined by ICP

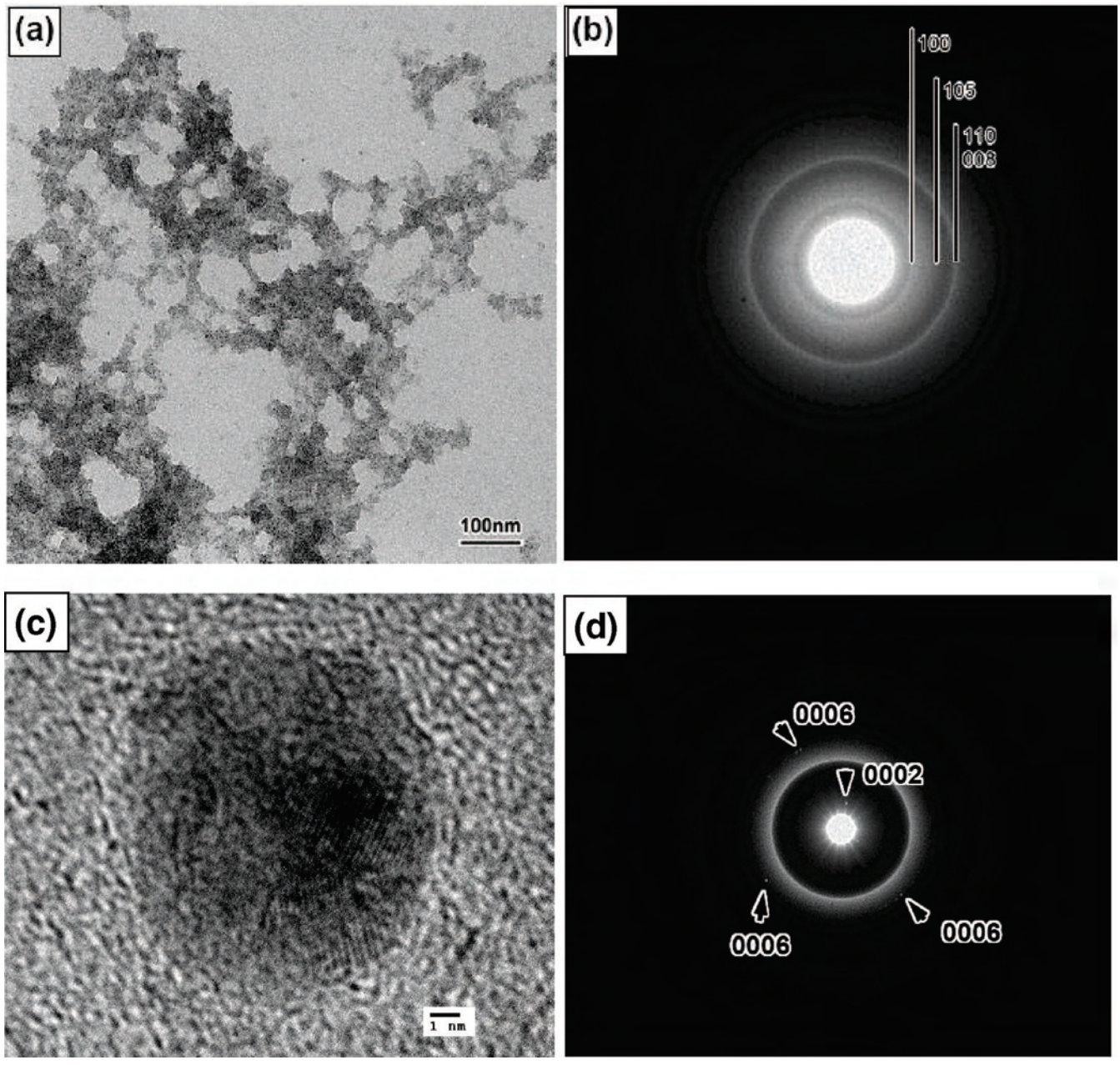

Figure 2. (a) Micrograph of an aggregated sample of MoS_2 nanoparticles and (b) corresponding selected area electron diffraction pattern. The three discernible diffuse rings can be indexed to peaks of the 2H-MoS_2 structure (as shown) or the 3R-MoS_2 structure [(101), (107), (110)/(113)]. After heating to 550 °C in situ, lattice fringes are evident at the edges of individual particles (c) and the electron diffraction pattern taken from a field of particles (d) reveals reflections corresponding to the interlamellar distances in 2H-MoS_2 (the (0002) and (0006) reflections of the hexagonal cell) or the (003) and (015) reflections from the 3R-MoS_2 structure.

(Desert Analytics) on a representative sample dissolved in 5% nitric acid (aqueous). The determined mass ratio of Mo to S was 42:26.

Optical Absorption Spectroscopy. Optical absorption measurements of MoS_2 nanoparticles in hexane were obtained on a Hewlett-Packard (HP) 8453 spectrophotometer. The dilute MoS_2 nanoparticle solutions in hexane were analyzed against a hexane blank in the region 200–600 nm.

Results and Discussion

MoS_2 nanoparticles were synthesized via the reaction of $Mo(CO)_6$ with elemental sulfur in a mixture of trioctylphosphine oxide (TOPO) and 1-octadecene (ODE) at 270, 300, or 330 °C, and the morphological and nanostructural characteristics of MoS_2 nanoparticles were elucidated by transmission electron microscopy (Figures 1 and 2). In all cases, small (<5 nm) spherical particles are prepared with standard deviations of 10–15% and the average size of the nanoparticles increases with increasing temperature, enabling the particle size to be tuned. However, the low contrast that is evident in the TEM images, and the need to defocus to image the particles, suggest that the majority of the as-prepared samples are poorly crystalline. In some cases, lattice fringes can be seen and indexed to either the 2H-MoS_2 structure (hexagonal) and/or the 3R-MoS_2 structure (rhombohedral) as shown in Figure S1 (Supporting Information), but these observations are rare. The diffuse rings observed in the selected area electron diffraction (SAED) conducted

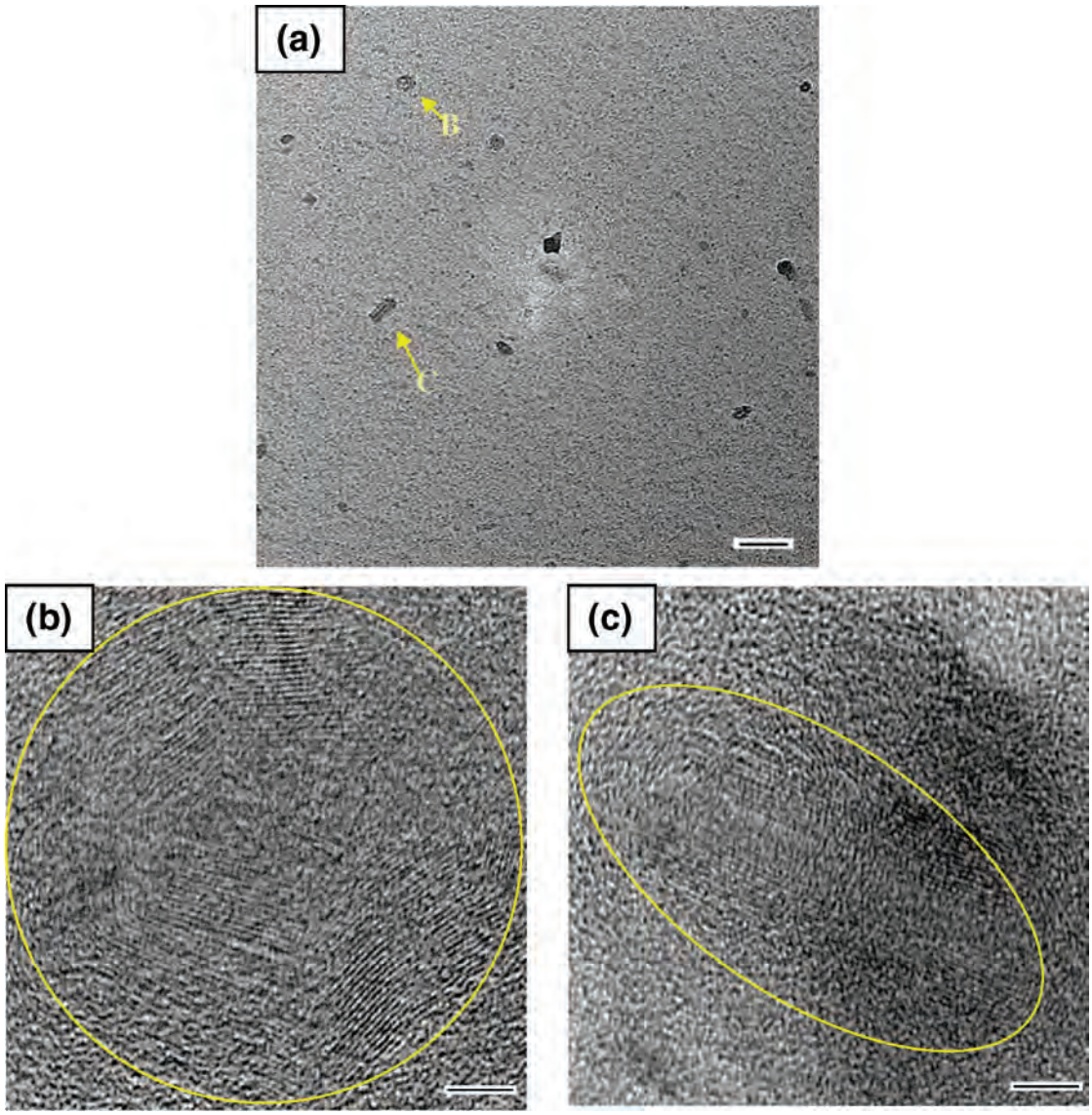

Figure 3. (a) Low magnification TEM image of onion- and tube-shaped MoS_2 nanoparticles. (b and c) High magnification TEM images of onion- (b) and tube-shaped (c) MoS_2 nanocrystals. The lattice fringes correspond to the (004) plane of 2H-MoS_2 (or the (006) plane of 3R-MoS_2). The scale bar is 100 nm for panel a and 5 nm for panels b and c.

on a field of aggregated particles (Figure 2a) are also suggestive of a poorly crystalline sample and index equally well to the 2H or 3R structures (Figure 2b). According to previous reports, 10–30 nm MoS_2 particles obtained from the use of *para*-xylene (a noncoordinating solvent) need 1 h of in situ heating in the TEM at 550 °C to crystallize the nanoparticles.[23] Accordingly, we heated our samples from 350 to 550 °C in the TEM and found a dramatic increase in the particle contrast as well as evidence of lattice fringes (Figure 2c), suggesting an improvement in crystallinity with heating. Additionally, spotted rings are evident in the electron diffraction acquired from a field of particles (Figure 2d) and can be indexed to the interlamellar distances in the 2H-MoS_2 structure (or the (003) and (015) of the 3R-MoS_2 structure). Spotted rings indicate that the field of particles captured in the diffraction experiment represents a wide range of crystallite orientations. This is often seen when the prepared crystallites are very small.

TEM-EDAX measurements were employed to probe the identity of the nanoparticles. The data reveal the presence of Mo, S, and P in the samples; however, because of overlap of the Mo and S peaks, quantitative data on the ratio of Mo:S cannot be obtained by this method. Accordingly, ICP analysis was performed and the data suggest a formulation of $MoS_{1.85}$. The presence of phosphorus noted in the EDS (ca. 16%) can be attributed to the presence of solvent TOPO groups binding to the surface of the particles. Assuming the ligands bind to metal atoms at the surface, the data is consistent with formation of particles consisting of a MoS_2 core with a Mo-rich surface that is bound by TOPO ligands.

Figure 3 shows the onion- and tube-shaped MoS_2 nanoparticles that arise when the ratio of ODE to TOPO is increased. As the amount of coordinating solvent is decreased, the particles are able to grow larger (average size near 40 nm) and, thus, presumably form closed-cage nanostructures to minimize dangling bonds at the particle edges.

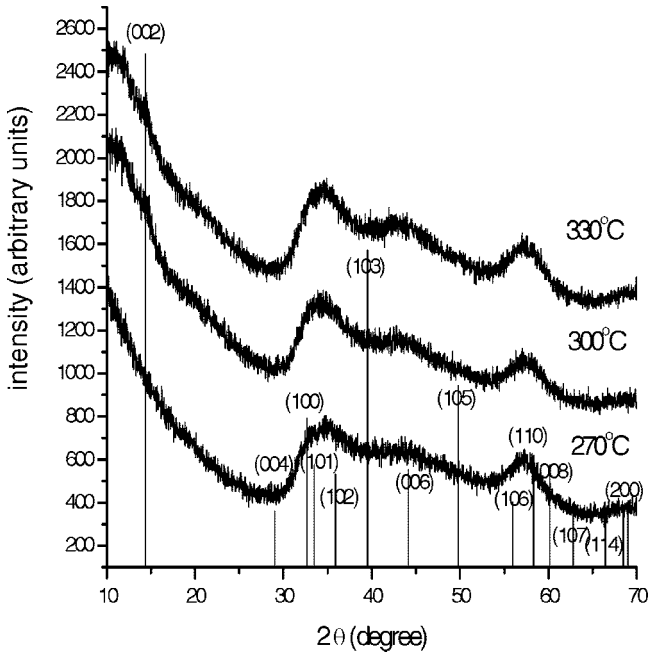

Figure 4. Powder X-ray diffraction patterns of sphere-shaped MoS_2 nanoparticles prepared at different synthetic temperatures (48 h heating). Vertical lines correspond to the 2H-MoS_2 structure, although the largely amorphous pattern matches the 3R-MoS_2 structure equally well.

The low contrast suggests a similarly low degree of crystallinity for the tubes and onions as was observed for the spherical particles. The spacing between lattice fringes (3.13 Å calculated value), corresponds to the (004) crystal plane of 2H-MoS_2 (3.07 Å) or the (006) reflection of 3R-MoS_2 (3.04 Å), suggesting that the fringes may correspond to individual sulfide layers within the MoS_2 slabs. It is not clear why the (002) reflection of the 2H-MoS_2 structure [or the (003) of the 3R-MoS2 structure] is not apparent, since this reflection is typically dominant, but this may be an indication of a large extent of destacking in the materials. The possibility that the multiwalled structures could be due to fullerenes was considered, but since the synthetic temperatures for the carbon based materials are in excess of 800 °C[25] and we are operating below 300 °C, we think this is unlikely.

Powder X-ray diffraction (PXRD) was employed to evaluate the extent of crystalline order in the samples (Figure 4). The patterns of spherical particles prepared at 270, 300, and 330 °C for 48 h were nearly identical and consisted of broad features that overlap with the expected pattern for either the 2H- or 3R-MoS_2 structures. Conspicuously absent are the (00*l*) reflections at ca. 6 Å that correspond to the interlayer distance along the *c*-axis in crystalline forms of MoS_2: the (002) reflection of the 2H-MoS_2 structure or the (003) reflection of the 3R-MoS_2 structure. In order to verify that the absence of (00*l*) reflections in the PXRD are not a consequence of preferred orientation, several PXRD sample preparation methods were explored, including solution deposition of nanoparticles (which might be expected to lead to preferred stacking of the basal planes) and shaken (not pressed) powder samples. In all cases, the PXRD patterns were essentially identical, with no (00*l*) reflection apparent, even after long scan times and background subtraction. This suggests an absence of order in the lamellar stacking. However, the XRD patterns of samples heated above 870 °C show the clear presence of this reflection (Supporting Information Figure S2) as well as a sharpening of the other reflections as the largely amorphous (destacked) as-prepared sample is transformed into crystalline MoS_2 with ordered stacking.

Performing the synthesis of spherical nanoparticles for shorter time periods (24 h) produced the same PXRD pattern, only with broader, less distinct features relative to samples heated for 48 h, suggesting an even lower degree of crystallinity in samples prepared at shorter times. Likewise, the patterns of onion- and tube-shaped MoS_2 nanoparticles produced when the concentration of coordinating solvent is lowered were indistinguishable from those for spherical particles. Despite observing lattice fringes in the TEM corresponding to the (004) planes of 2H-MoS_2 (or the (006) planes of 3R-MoS_2), no clearly defined (00*l*) reflections were obtained in the PXRD, suggesting little or no ordered stacking. However, since small particles invariably accompany these larger features, we cannot definitively assign the PXRD pattern to the tubes and onions.

In contrast to synthetic methods reported elsewhere,[8,10,23] the as-obtained MoS_2 products from the arrested precipitation reactions in TOPO showed excellent dispersity in a variety of nonpolar organic solvents, such as toluene, pyridine and chloroform. This can be attributed to the presence of capping TOPO ligands that confer stability against aggregation and precipitation while the long alkyl chains favor dispersion in relatively nonpolar solvents, as is well established for other nanoparticle systems prepared by this strategy.[26] The inability to disperse the particles in polar solvents strongly argues that the ability to disperse is not a simple function of particle size but is highly dependent on the surface functionality. When stored under air-free conditions, the MoS_2 nanoparticles are stable for at least several weeks in solution (i.e., no precipitation occurs) and should be suitable for depositing onto supports for catalytic studies.

Despite the expectation of strong quantum confinement effects, optical absorption spectra are essentially featureless, with a broad absorption onset at 340 nm (Supporting Information Figure S3). These data are not unlike the spectra reported for MoS_2 nanoparticles prepared from dissolution of bulk phases in acetonitrile[27] but are lacking in the specific features observed for materials prepared by inverse micelle routes.[20–22] A more rigorous purification protocol and/or high temperature crystallization may enable the intrinsic quantum confinement effects to be observed.[21] Despite the fact that these samples are not optically interesting, the amorphous nature of the material that impairs formation of a defined band gap may actually enhance the catalytic activity due to a larger number of available rim sites.[11,12]

(25) Markovic, Z.; Todorovic-Markovic, B.; Mohai, I.; Farkas, Z.; Kovats, E.; Szepvolgyi, J.; Otasevic, D.; Scheier, P.; Feil, S.; Romcevic, N. *J. Nanosci. Nanotechnol.* **2007**, *7*, 1357–1369.

(26) Peng, Z. A.; Peng, X. *J. Am. Chem. Soc.* **2001**, *123*, 183–184.

(27) Peterson, M. W.; Nenadovic, M. T.; Rajh, T.; Herak, R.; Micic, O. I.; Goral, J. P.; Nozik, A. J. *J. Phys. Chem.* **1988**, *92*, 1400–1402.

Acknowledgment. We thank Dr. Sam Shinozaki for assistance with the transmission electron microscopy. This research was supported by a grant from NSF (DMR-0094273) and the donors of the Petroleum Research Fund, administered by ACS (43550-AC10). The electron microscopy work was performed at the WSU Central Instrumentation Facility on a JEOL 2010 FasTEM purchased under NSF grant DMR-0216084.

Supporting Information Available: High resolution TEM image of a single as-prepared MoS_2 nanoparticle showing lattice fringes; X-ray powder diffraction of a MoS_2 nanoparticle sample heated ex situ; optical absorbance spectrum for a sample of MoS_2 nanoparticles. This material is available free of charge via the Internet at http://pubs.acs.org.

IC701020S